Nucleon Magnetic Moments in Light-Front Models with Quark Mass Asymmetries

W. R. B. de Araújo[a], L. A. Trevisan[b], T. Frederico[a], L. Tomio[c], and A. E. Dorokhov[d]

[a] *Departamento de Física, Instituto Tecnológico de Aeronáutica, Centro Técnico Aeroespacial, 12.228-900, São José dos Campos, SP, Brazil*

[b] *Departamento de Matemática, Universidade Estadual de Ponta Grossa, 84030-000, Ponta Grossa, PR, Brazil*

[c] *Instituto de Física Teórica, UNESP, Rua Pamplona 145, 01405-900, São Paulo, Brazil*

[d] *Bogoliubov Laboratory of Theoretical Physics, JINR, Dubna, 141980, Russia*

Received on 6 October, 2003

We show that the systematic inconsistence found in the simultaneous fit of the neutron and proton magnetics moments in light-front models, disappears when one allows an asymmetry in the constituent quark masses. The difference between the constituent quarks masses is an effective way to include in the nucleon model the effect of the attractive short ranged interaction in the singlet spin channel.

1 Introduction

It is well known that in light-front models of the nucleon with point-like quarks, the proton and neutron magnetic moments are not reproduced simultaneously without further assumptions [1, 2, 3, 4]. More recently, it was shown that in several nucleon light-front models, the proton and neutron magnetic moments are strongly correlated [5]. The detailed form of the correlation was found manly dependent on the relativistic spin coupling scheme. In Ref. [5], the coupling of the quark to the nucleon fields was formulated through an effective Lagrangian, which dials the different relativistic spin coupling schemes. Although some of the previous calculations [2, 3, 4] were performed within the Bakamjian-Thomas construction (BT) [6] of the nucleon light-front wave function, the results found for the magnetic moments were consistent with those obtained with an effective Lagrangian with mixed scalar plus gradient coupling [5]. In fact, it was pointed out that the BT and the mixed scalar plus gradient effective Lagrangian constructions of the spin wave function provides the same form when the free mass of the three-quark system is identified with the nucleon plus momentum component [7].

It was shown by [4], that the pion and the nucleon light-front wave functions present hard-constituent components, i.e., high momentum tails, above 1 GeV/c, due to the short-range attractive part of the interaction in the spin singlet state, as taken from the Godfrey and Isgur model[8]. Consequently, the nucleon wave function can exhibit a higher momentum tail related to short ranged physics of the constituent quarks. However, the high momentum tail in the nucleon light-front wave function is unable to breakdown the strong correlation between the nucleon magnetic moments, while the electromagnetic form factors presents sharply different characteristics at moderate momentum transfers ($\sim 2-3$ GeV), as we are going to show through some examples.

In the present work, we study a possibility to improve light-front models of the nucleon with point-like quarks, in order to obtain a simultaneous fit of the neutron and proton magnetic moments. We introduce a difference between the constituent quarks masses in the nucleon, which is understood to be an effective way to include in the model the effect of the attractive short ranged spin-spin force in singlet channel. The origin of the attraction in the singlet channel can be related to the one-gluon hyperfine interaction or other short ranged effects, like the instanton induced interaction (see discussion in [9]). In the proton, the quark d sees a more attractive field than the up-quarks. The uu quark pair is in the triplet spin state while the d quark has opposite spin projection and consequently the spin-spin attraction is stronger for d. This effect can be simulated by a smaller mass for the d-quark in the proton[10]. For the same reason, in the neutron , u would be lighter than d. Here, we take into account the effect of the different quark masses in the computation of the nucleon magnetic moments and we show that the disagreement with the data can be qualitatively solved.

This paper is organized as follows. In Sec. 2, we briefly present the nucleon wave function model. In Sec. 3, we review shortly the calculation of the nucleon electromagnetic form factors. The results of our calculations are shown in Sec. 4, and the summary in Sec. 5.

2 The Nucleon Model

The spin part of the nucleon light-front wave function is described with an effective Lagrangian for the N-q coupling,

which is written as[5],

$$\mathcal{L}_{\rm N-3q} = \alpha m_N \epsilon^{lmn} \overline{\Psi}_{(l)} i\tau_2\gamma_5 \Psi^C_{(m)} \overline{\Psi}_{(n)} \Psi_N + (1-\alpha)\epsilon^{lmn} \overline{\Psi}_{(l)} i\tau_2\gamma_\mu\gamma_5 \Psi^C_{(m)} \overline{\Psi}_{(n)} i\partial^\mu \Psi_N + H.C \quad (1)$$

where τ_2 is the isospin matrix, the color indices are $\{l, m, n\}$ and ϵ^{lmn} is the totally antisymmetric symbol. The conjugate quark field is $\Psi^C = C\overline{\Psi}^\top$, where $C = i\gamma^2\gamma^0$ is the charge conjugation matrix; α is a parameter to dial the spin coupling parameterization.

The momentum component of the wave function is chosen as the harmonic and power-law forms [11, 12], with one or two scales:

$$\Psi_{\rm HO} = N_{\rm HO}\left[\exp(-M_0^2/2\beta^2) + \lambda\exp(-M_0^2/2\beta_1^2)\right] ,$$
$$\Psi_{\rm Power} = N_{\rm PW}\left[(1+M_0^2/\beta^2)^{-p} + \lambda(1+M_0^2/\beta_1^2)^{-p}\right] . \quad (2)$$

The normalization is determined by the proton charge. The width parameters, i.e., the characteristic momentum scales of the wave function are β and β_1. M_0 is the free mass of the three-quark system. The one scale models have $\lambda = 0$. We observe that, the lower momentum scale of the wave function, β, is essentially determined by the static observables and the higher one is related to the possible zero of G_{Ep} at square momentum transfer, $q^2 \sim 7.7$ GeV^2, as indicated by the recent experiments [13, 14].

The power-law fall-off from general QCD arguments has a value of $p = 3.5$ in Eq.(2) [12, 11]. From the point of view of the static electroweak observables, the value of p does not present an independent feature at least in the static observables, which are strongly correlated, as long as $p > 2$ [5, 12]. Here $p = 3$ is chosen without any loss of generality in our analysis, as different momentum components of the wave function leads to the same correlation between the nucleon magnetic moments [5]. Furthermore, we will show that the two-scale power-law model also preserves the correlation curve between the magnetic moments.

3 Nucleon electromagnetic current

The nucleon electromagnetic form factors are derived from the valence component of the light-front wave function using the plus component of the current ($J^+_N = J^0_N + J^3_N$) for momentum transfers satisfying the Drell-Yan condition $q^+ = q^0 + q^3 = 0$. The contribution of the Z-diagram is minimized in a Drell-Yan frame while the wave function contribution to the current is maximized (see [15, 16] and references therein). We use the Breit-frame, where the four momentum transfer $q = (0, \vec{q}_\perp, 0)$ is such that $(q^+ = 0)$ and $\vec{q}_\perp = (q^1, q^2)$, satisfying the Drell-Yan condition.

The matrix elements of the current $J^+_N(q^2)$ are computed in the nucleon light-front spinor basis in the Breit-frame constrained by the Drell-Yan condition, which is written as [2, 5]:

$$F_{1N}(q^2) = \frac{1}{\sqrt{1+\eta}}\langle\uparrow|J^+_N(q^2)|\uparrow\rangle ,$$
$$F_{2N}(q^2) = \frac{1}{\sqrt{\eta}\sqrt{1+\eta}}\langle\uparrow|J^+_N(q^2)|\downarrow\rangle , \quad (3)$$

where F_{1N} and F_{2N} are the Dirac and Pauli form factors, respectively and $\eta = -q^2/4m_N$. The momentum transfer in the Breit-frame was chosen along the x-direction, i.e., $\vec{q}_\perp = (\sqrt{-q^2}, 0)$.

The electric and magnetic form factors (Sachs form factors) are given by:

$$G_{EN}(q^2) = F_{1N}(q^2) + \frac{q^2}{4m_N^2}F_{2N}(q^2) ,$$
$$G_{MN}(q^2) = F_{1N}(q^2) + F_{2N}(q^2) , \quad (4)$$

where $N = n$ or p. Here $\mu_N = G_{MN}(0)$ and $\kappa_N = F_{2N}(0)$ are the magnetic and anomalous magnetic moments, respectively. The charge mean square radius is $r^2_N = 6\frac{dG_{EN}(q^2)}{dq^2}|_{q^2=0}$.

The macroscopic matrix elements of the current are identified with the microscopic ones, which are calculated within our relativistic model of the nucleon. It is assumed the dominance of the valence component of the wave function in the electromagnetic observables. The microscopic matrix elements of the current are derived using the effective Lagrangian, Eq.(1), within the light-front impulse approximation which is represented by four three-dimensional two-loop diagrams [5], which embodies the antisymmetrization of the quark state in the wave function. The detailed form of the expressions used in our calculations were discussed thoroughly in our previous works[5].

TABLE I. Parameters of the power-law model with scalar quark spin coupling ($\alpha = 1$). The magnetic moments are shown in the last two columns.

case	β[MeV]	β_1[MeV]	λ	$\mu_n(\mu_N)$	$\mu_p(\mu_N)$
(a)	616	5720	5×10^{-5}	-1.51	2.72
(b)	616	5720	-5×10^{-5}	-1.66	2.86
(c)	1034	-	-	-1.51	2.78
Exp.	-	-	-	-1.91	2.79

4 Numerical Results

The parameters of the present two-scale model of the nucleon light-front wave function are the constituent quark mass, the momentum scales β and β_1, and the relative weight λ (see Eq.(2)). We use, as before [4, 8, 5], a constituent quark mass value of $m = 0.22$ GeV in the numerical evaluation of the form factors and $p = 3$ for the power-law model. The relative weight parameter λ, the momentum scales β and β_1 of the different models are found from the proton magnetic momentum and the experimental ratio $\mu_p G_{Ep}/G_{Mp}$ [13, 14]. We are going to use previous results [5] with one scale models with Gaussian and power-law forms, to compare with the new two-scale model.

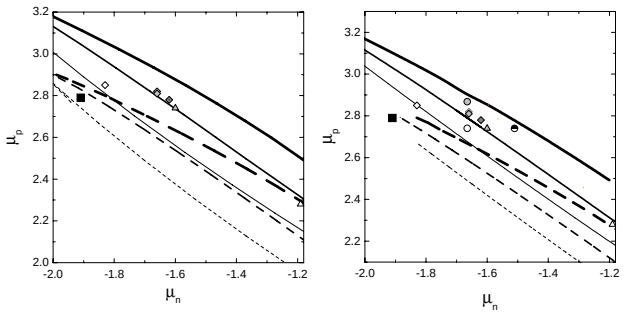

Figure 1. Proton magnetic moment as a function of the neutron magnetic moment for several models. In the left and right frames are presented results for h.o. and power-law models, respectively. Results of one scale models for $\alpha = 1$ (thick solid line), $\alpha = 1/2$ (solid line) and $\alpha = 0$ (thin solid line). Correction of the one scale model results due to the quark mass difference for $\alpha = 1$ (thick dashed line), $\alpha = 1/2$ (dashed line) and $\alpha = 0$ (dotted line). Results for two-scale models of Table I: (a) (circle with black dot) and (b) (gray circle). Results of BT calculations from [3] (diamonds) and from [4] (triangles). Experimental data (full square).

In Fig. 1, we show the correlation between the magnetic moments, μ_p and μ_n for several different models. First, we compare the calculations performed within the BT framework [3, 4] with results obtained with one-scale models [5]. The calculations for the one-scale harmonic and power-law forms were done for scalar coupling $\alpha = 1$, scalar coupling plus gradient coupling $\alpha = 1/2$ and gradient coupling $\alpha = 0$ in Eq.(1). The parameter β was changed to produce the continuous curves shown in Fig. 1.

We observe that the nucleon magnetic moments obtained within the BT scheme [3, 4] are consistent with the effective Lagrangian model results for $\alpha = 1/2$ in Eq.(1), with only one exception. It is reasonable to expect that the BT and $\alpha = 1/2$ spin coupling schemes produce consistent results as they are qualitatively similar in respect to the spin component of the wave function.

In the relativistic spin component of the nucleon wave function generated by $\alpha = 1/2$, the Melosh rotations have the arguments defined by the kinematical momentum of the quarks in the nucleon rest frame. The difference with the BT construction of the spin coupling coefficients appears only in the argument of the Melosh rotations which are defined for a system of three-free particles [7]. As the constituent quark masses are sizeable in respect to the nucleon inverse size, one expects the similarity between the two spin coupling schemes, which explains our findings.

We performed calculations of the nucleon electromagnetic form factors for the power-law wave function with two scales and scalar coupling ($\alpha = 1$) for the parameters presented in Table I. The choice of the scalar form of spin coupling is motivated by the finding that the neutron square charge radius, electric form factor and magnetic moment are fitted simultaneously with one scale models [5].

In order to make broader choices of parameters, we have used λ positive (a) and negative (b). In the case of $\lambda > 0$, the parameters are found by fitting approximately the proton magnetic moment and the proton ratio $\mu_p G_{Ep}/G_{Mp}$ from the recent experiments [13, 14]. (Later on, we will present results for the form factors.) In Table I, we also present a one scale power-law model (c) which gives the same neutron magnetic moment as model (a). The proton magnetic moments in models (a) and (c) differ only at the level of 5%, therefore the strong correlation between μ_p and μ_n found for one-scale models are valid for the case of two-scales wave functions. Even with the change of sign in λ from positive to negative the results are consistent with the correlation plot as one sees in Fig. 1.

The next point in the analysis of the nucleon magnetic moments is to introduce in the model an asymmetry in the quark masses as we have discussed before. The quark d effectively could present a smaller mass in the proton, $m_u - m_d = \delta_m > 0$, while in the neutron $m_d - m_u = \delta_m$. Using a nonrelativistic calculation of the nucleon magnetic moments in lowest order in δ_m, one easily finds that the shift in the nucleon magnetic moments are given by:

$$\delta\mu_p = -\frac{2\delta_m}{3m} \quad , \quad \delta\mu_n = \frac{4\delta_m}{m} \; ; \tag{5}$$

where m is the mass of the heaviest quark in the proton or neutron. The shifts in μ_p and μ_n tend to decrease both values, which can lower the theoretical curves presented in Fig. 1 toward the experimental point. Indeed, for each one scale-model calculation presented in Fig. 1, the correction from Eq.(5) is applied with a quark mass difference of about 15%, which result in agreement with experimental values.

With the sake to be complete, we show in Figs. 2 and 3 the proton and neutron electromagnetic form factors for the power-law wave functions with two scales (a) and (b), compared to the results of the one-scale model (c) for the scalar quark-nucleon coupling in the effective Lagrangian.

In Fig. 2, the calculations for $\mu_p G_{Ep}/G_{Mp}$ ratio are compared to the experimental data [13, 14]. The two scale wave function model (a) with $\lambda > 0$ presents a nice fit to the ratio data showing how to overcome the limitation found with one-scale models, for which the zero of $\mu_p G_{Ep}/G_{Mp}$ appeared at to low momentum transfers [5], as is also seen for the one-scale model (c). It is interesting to observe that when the sign of λ is changed, the respective curve is well above of the experimental data [17]. The proton magnetic form factor obtained with the two-scale model (a) and the the one-scale model (c) are close, indicating a strong dominance of the value of the neutron magnetic moment in this observable. The two-scale model (b) which presents a better value of μ_n approaches the data for $G_{Mp}(q^2)$.

In Fig. 3, the results for the neutron electric form factor show a strong dependence with the neutron magnetic moment. The models (a) and (c), which have the poorest value of μ_n strongly disagree with the data, while the model (b) with a better value for μ_n appears to be more consistent with the experimental values for G_{En}. This finding is consistent with the calculations of Ref. [5] performed for one-scale models with $\alpha = 1$ and β chosen to fit μ_n, where a good agreement with the data for G_{En} was found. Thus, there is a strong dependence of the theoretical neutron electric form factor with μ_n.

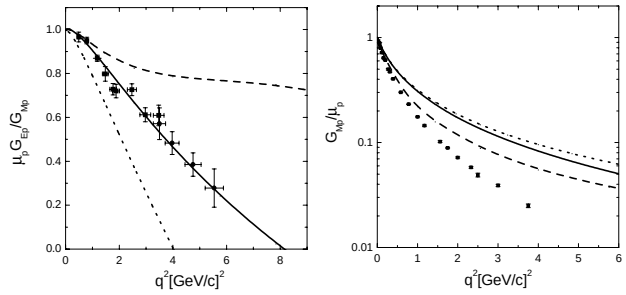

Figure 2. Proton form factor ratio $\mu_p G_{Ep}(q^2)/G_{Mp}(q^2)$ and magnetic form factor as a function of the square momentum transfer. Results for power-law models with $\alpha = 1$: (a) (solid line), (b) (dashed line) and (c)(dotted line), see Table I. Experimental data in left frame from Refs. [13, 14]. Experimental data in right frame from Ref. [17].

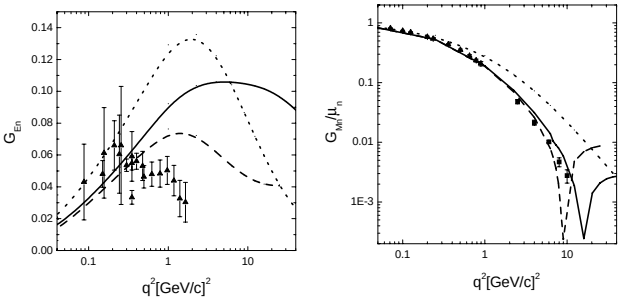

Figure 3. Neutron electric and magnetic form factors as a function of the square momentum transfer. Theoretical curves labeled as in Fig. 2. The triangles and the squares are the experimental data from the compilation of Ref. [18] and Ref.[19], respectively.

Finally, the magnetic neutron form factor for the two scale models (a) and (b) present a new feature: an unexpected zero at high momentum transfer, above $10GeV^2$. In general, the one scale model do not have a zero in G_{Mn}, as seen for the model (c). In our study, we observe that two-scale model (a) for which $\lambda > 0$ shows a zero for higher momentum transfers when compared model (b) with $\lambda < 0$. In both cases, we observe that the two-scale models present a better fit to the experimental data than the one-scale model.

5 Summary

Our study indicates that the simultaneous fit of nucleon magnetic moments in light-front models with point-like quarks needs some further assumptions. Here, we have shown that considering a difference in the quark masses of about 15%, the correlation between the proton and the neutron magnetic moments goes through the experimental values. We have also shown new features of the two-scale models with a high momentum tail, which is able to reproduce the recent data of $\mu_p G_{Ep}/G_{Mp}$ and presents a zero in the neutron magnetic form-factor around 10 GeV^2.

Acknowledgments

We thank FAPESP, CNPq, LCCA/USP and CENAPAD/UNICAMP. AED thanks for partial support from RFBR (Grants nos. 02-02-16194, 03-02-17291, 04-02-16445), INTAS (no. 00-00-366).

References

[1] W. Konen and H.J. Weber, Phys. Rev. D**41**, 2201 (1991).

[2] P. L. Chung and F. Coester, Phys. Rev. D**44**, 229 (1991).

[3] F. Schlumpf, Phys. Rev. D**47**, 4114 (1993).

[4] F. Cardarelli, I.L. Grach, I.M. Narodetskii, G. Salmè and S. Simula, Phys. Lett. B**349**, 393 (1995); F. Cardarelli, E. Pace, G. Salmè and S. Simula, Phys. Lett. B**357**, 267 (1995); Few Body Syst. Suppl. **8**, 345 (1995).

[5] W.R.B. de Araújo, E.F. Suisso, T. Frederico, M. Beyer, and H.J. Weber, Phys. Lett. B**478**, 86 (2000); E. F. Suisso, W.R.B. de Araújo, T. Frederico, M. Beyer, and H.J. Weber, Nucl. Phys. A**694**, 351 (2001).

[6] B. Bakamjian and L. H. Thomas, Phys. Rev. **92**, 1300 (1953).

[7] W.R.B. de Araújo, M. Beyer, T. Frederico, and H.J. Weber, J. Phys. G**25**, 1589 (1999).

[8] S. Godfrey and N. Isgur, Phys. Rev. D**32**, 189 (1985).

[9] T. Frederico, H.-C. Pauli, and S.-G. Zhou, Phys. Rev. D**66**, 054007 (2002); Phys. Rev. D**66**, 116011 (2002).

[10] Luis Augusto Trevisan, Tese de Doutorado, Instituto de Física Da Universidade de São Paulo, 1997.

[11] S.J. Brodsky, H.-C. Pauli, and S.S.Pinsky, Phys. Rep. **301**, 299 (1998).

[12] S. J. Brodsky and F. Schlumpf, Phys. Lett. B**329**, 111 (1994); Prog. Part. Nucl. Phys. **34**, 69 (1995).

[13] M. K. Jones et al. [Jefferson Lab Hall A collaboration], Phys. Rev. Lett. **84**, 1398 (2000).

[14] O. Gayou et al., Phys. Rev. Lett. **88**, 092301 (2002).

[15] J.P.B.C de Melo, H.W. Naus, and T. Frederico, Phys. Rev. C**59**, 2278 (1999).

[16] B.L.G. Bakker, H.-M. Choi, and C.-R. Ji, Phys. Rev. D**63**, 074014 (2001).

[17] W. Bartel et al., Nucl. Phys. **58**, 429 (1973).

[18] H. Gao, Int. J. Mod. Phys. E**12**, 1 (2003); and references therein.

[19] S. Rock et. al., Phys. Rev. Lett. **49**, 1139 (1982).